Available online at www.sciencedirect.com
SCIENCE DIRECT®
Acta Materialia 52 (2004) 4351–4362
Acta MATERIALIA
www.actamat-journals.com

Origin of abnormal multi-stage martensitic transformation behavior in aged Ni-rich Ti–Ni shape memory alloys

Genlian Fan [a,b], Wei Chen [a,c], Sen Yang [a,d], Jinhua Zhu [b], Xiaobing Ren [a,b,e,*], Kazuhiro Otsuka [e]

[a] *Multi-disciplinary Materials Research Center, Xi'an Jiaotong University, Xi'an 710049, China*
[b] *State Key Laboratory for Mechanical Behaviour of Materials, Xi'an Jiaotong University, Xi'an 710049, China*
[c] *State Key Laboratory of Electrical Insulation for Power Equipment, Xi'an Jiaotong University, Xi'an 710049, China*
[d] *Department of Physics, Xi'an Jiaotong University, Xi'an 710049, China*
[e] *Materials Physics Group, National Institute for Materials Science, 1-2-1 Sengen, Tsukuba 305-0047, Ibaraki, Japan*

Received 7 April 2004; received in revised form 31 May 2004; accepted 2 June 2004
Available online 24 June 2004

Abstract

After aging Ni-rich Ti–Ni alloys exhibit finely dispersed Ti_3Ni_4 particles embedded in B2 matrix. Under such condition the B2 matrix normally undergoes two-stage martensitic transformation B2-R-B19′. However, there is also evidence of three-stage transformation. The origin of such abnormal three-stage transformation remains controversial. In the present study, we made a comparative study between single crystals and corresponding polycrystals and found that all single crystals exhibit normal two-stage transformation, being independent of Ni content. By comparison, polycrystals with low Ni content (50.6Ni) show three-stage transformation, but those with high Ni content (51.5Ni) again exhibit normal two-stage transformation. These new findings are consistent with a simple scenario that different transformation behaviors are a result of competition between preferential grain-boundary precipitation of Ti_3Ni_4 particles and a tendency for homogeneous precipitation when supersaturation of Ni is large. This is a natural consequence of the nucleation kinetics of supersaturated solid solutions *in polycrystalline state*. The above scenario not only explains the abnormal three-stage transformation but also the normal two-stage transformation.

Keywords: Shape memory alloy; Ti–Ni; Single crystal; Martensitic transformation; Aging; Precipitation

1. Introduction

Martensitic transformation in Ti–Ni shape memory alloys has attracted much attention in past decades since it is the origin of the unique shape memory effect and superelasticity [1,2]. Usually a one-stage transformation B2-B19′ occurs in solution-treated Ni-rich Ti–Ni alloys and a two-stage transformation B2-R-B19′ occurs after additional aging treatment, which creates finely dispersed Ti_3Ni_4 precipitates in B2 matrix [2]. The change from one-stage transformation to two-stage transformation can be understood by considering that R-phase is another potential martensite candidate and the relative preference of the R-phase over B19′ martensite in the presence of fine particles. This is because Ti_3Ni_4 particles produce a strong resistance to the formation of B19′, which is associated with a large lattice deformation; but they have much less resistance to the formation of R-phase, which is associated with a significantly smaller lattice deformation [3]. Therefore, the presence of Ti_3Ni_4 particles favors the formation of R-phase and it requires further cooling to form B19′ martensite. As a consequence, martensitic transformation occurs in two steps: B2-R-B19′.

However, surprisingly a three-stage martensitic transformation in aged Ni-rich Ti–Ni alloys was reported from time to time in the literature [4–17]. No new kind of martensite was detected by diffraction studies

* Corresponding author. Tel.: +81-29-859-2731; fax: +81-29-859-2701.
E-mail address: Ren.Xiaobing@nims.go.jp (X. Ren).

1359-6454/$30.00 © 2004 Acta Materialia Inc. Published by Elsevier Ltd. All rights reserved.
doi:10.1016/j.actamat.2004.06.002

[10,11]. It is unclear why two kinds of transformations (B2-R-B19′) can result in three DSC peaks.

This abnormal transformation behavior has attracted much interest in recently years. Several explanations have been given based on different experimental observations.

(1) Bataillard et al. [8,11] suggested that three-stage transformation stems from an inhomogeneous stress distribution in the B2 matrix around Ti_3Ni_4 particles. Such stress inhomogeneity arises from the coherency between the precipitates and B2 matrix. They proposed that in such a stress-inhomogeneous system R-phase transformation occurs in one step but R-B19′ transformation occurs in two steps, corresponding to the high stress region (near precipitate) and low stress region (away from precipitate), respectively. Apparently, this mechanism is based on small-scale stress inhomogeneity around Ti_3Ni_4 particles and thus it follows that three-stage transformation should also occur even in single crystal of Ti–Ni.

(2) Khalil-Allafi et al. [12] performed a systematic investigation of the evolution of transformation behavior with aging temperature and time by means of DSC measurement. They proposed that three-stage transformation is due to the composition inhomogeneity in matrix B2 phase between Ti_3Ni_4 particles. Such composition inhomogeneity is a result of the kinetics of precipitation process out of a supersaturated solid solution. They suggested that the Ti–Ni system with composition inhomogeneity between Ti_3Ni_4 particles would create one B2-R transformation and two R-B19′ transformation, the latter corresponding to the transformation at low Ni region (near Ti_3Ni_4) and high Ni region (away from Ti_3Ni_4), respectively. Apparently, this mechanism is also based on small-scale (chemical) inhomogeneity between Ti_3Ni_4 particles; it suggests three-stage transformation should also occur in Ti–Ni single crystals.

(3) Khalil-Allafi et al. [13] and Dlouhy et al. [14] studied microstructures of Ni-rich Ti–Ni alloys after aging treatment and found that precipitation of small lenticular Ti_3Ni_4 precipitates occurs preferentially at grain boundaries. The major part of the grain interior is free of precipitates. They suggested from their in situ TEM observation that the first DSC peak corresponds to the formation of R-phase at grain boundary regions containing precipitates and the second DSC peak corresponds to the formation of B19′ in the same regions, the third distinct peak corresponds to B2-B19′ transformation in precipitate-free grain interior regions. This mechanism points out the importance of large-scale inhomogeneity in precipitation between grain boundary and interior. Nevertheless, it follows from this scenario that after cooling to the end of second transformation the grain interior will still be in B2 state. But recent neutron diffraction study (which monitors bulk behavior) and TEM study [15] of the same sample yielded contradicting results: B2 is almost absent at such temperature and grain interior is B19′ rather than B2 (Ref. [15] seems to have neglected the small second transformation peak on cooling).

Adding to above controversies, there is even a well-observed fact that is hard to explain by any proposed mechanism. That is, all the above explanations imply that three-stage transformation is always the case, as the inhomogeneity (due to stress distribution, composition inhomogeneity and grain boundary effect) required by the above mechanisms is always present. But as a matter of fact, the majority of the reported DSC curves show normal two-stage transformation (B2-R-B19′), rather than the three-stage transformation. Therefore, there is a need to explain why three-stage transformation occurs only under certain condition and why not under other conditions. Furthermore, it was recently found that the appearance of three-stage transformation depends on heat treatment atmosphere [16]. Normal two-stage rather than three-stage transformation occurs when the specimens are protected from oxidation by Ti and Zr getter during solution-treatment. This result is also difficult to explain by existing mechanisms.

Therefore, despite the recent progress the understanding to the curious three-stage transformation in Ti–Ni alloys is still in an early stage and there is no theory that can explain all existing data, in particular about why in some cases two-stage transformation occurs while in other cases three-stage transformation occurs. It seems that the additional transformation does arise from certain inhomogeneity, as proposed by previous mechanisms [8,11–14]; but it is unclear what kind of inhomogeneity is responsible and why under certain conditions (composition or heat-treatment atmosphere) such inhomogeneity does not play a role and yield a normal two-stage transformation behavior. In order to give a unified explanation to both the abnormal three-stage transformation and the normal two-stage transformation in Ni-rich Ti–Ni alloys, in the present study we carefully designed our experiment and chose suitable samples. Firstly, we used single crystals of Ti–Ni alloys, for which the influence of grain boundary can be excluded. If local inhomogeneity (either in stress or composition) around Ti_3Ni_4 precipitates is responsible for the abnormal three-stage transformation behavior, one can expect a three-stage transformation in these single crystal samples after aging. This is a critical test to mechanisms 1 and 2. Secondly, in order to understand the effect of grain boundary on the transformation behavior, we changed our single crystals into polycrystals by cold working and followed by recrystallization treatment at high temperature. We name such polycrystalline samples "artificial polycrystals" hereafter. This ensures a strict comparability of the results between single and polycrystals, as the chemical composition can

be kept exactly the same. Thirdly we prepared two sets of Ti–Ni single/artificial-polycrystal samples with different composition (50.6Ni and 51.5Ni), in order to investigate the effect of Ni content. As will be seen in the following, such a systematic investigation yields a simple and unified explanation to both three-stage transformation behavior and normal two-stage transformation behavior, as well as the composition dependence of the behavior.

2. Experimental

Two kinds of Ni-rich single crystals, Ti–50.6at.%Ni and Ti–51.5at.%Ni, were used in the present investigation. Ni content of the samples were estimated from their transformation temperatures and complemented by electron probe micro-analysis.

The single crystals were spark-cut into small pieces (about $3 \times 3 \times 1$ mm^3). The samples were mechanically polished and chemically etched in order to remove the affected surface layer, and then sealed into quartz tubes filled with low-pressure argon to avoid oxidization during heat treatment. All the sealed samples were solution-treated at 1273 K for 1 h and water quenched to obtain supersaturated homogeneous solid solution, and then aged at 673, 723 and 773 K for different aging time from 1 to 150 h. After the above heat treatment the samples were again chemically etched to remove the surface layer that might be slightly oxidized during heat treatment. The etching agent consisted of hydrofluoric acid, nitric acid and water in the proportion of 10:40:50 in volume.

A differential scanning calorimeter (DSC) of type 822^e from METTLER TOLEDO was used to measure the phase transformation temperature. DSC samples have a mass between 10 and 50 mg. Heating and cooling rate were 10 K/min.

In order to make a reliable comparison between the behavior of single crystals and polycrystals, we made "polycrystals" out of the single crystals of the same composition by the following method. Firstly, the above single crystal samples were heavily cold-compressed (about 50%) to introduce high density of dislocations. The deformed samples were then sealed in quartz tubes and recrystallized at 1273 K for 1 h (except the sample for Fig. 3(c); that sample was solution-treated for 6 h to make the grain size more homogeneous). The recrystallization treatment changes the deformed samples into polycrystals with a grain size of about 50 μm. These "artificial polycrystals" were heat-treated in the same way as done for single crystals in the sealed quartz tube, and the aging conditions were also the same as those for single crystals.

Samples for transmission electron microscopy were mechanically polished down to about 0.15 mm and finally electropolished using a twin-jet apparatus at 250 K. The electrolytic solution consists of 5 vol% $HClO_4$ and 95 vol% CH_3CH_2OH. TEM observation with JEM-200CX and 2010 was performed at room temperature (about 298 K).

3. Experimental results

3.1. DSC results of single crystals

In this section, we report the DSC curves for single crystals. The DSC curves of Ti–50.6Ni and Ti–51.5Ni are shown in Figs. 1 and 2, respectively. After solution treatment (1273 K, 1 h) followed by quenching into water, the 50.6Ni single crystal (Fig. 1(a)) undergoes one stage B2-B19′ transformation with a hysteresis of 40 K. For 51.5Ni single crystal (Fig. 2(a)) the DSC curves show no distinct peak because the transformation temperature is out of the DSC measurement window.

Now it is interesting to see the DSC results of Ti–Ni single crystals after aging treatment, as such data can be a crucial test to three-peak mechanisms based on small-scale stress or composition inhomogeneity around Ti_3Ni_4 particles. For 50.6Ni single crystals that were solution-treated and aged at 723 K for different time, DSC curves show two distinct exothermic peaks on cooling disregard of aging time. On heating there are two endothermic peaks when aged for short time (1 h) and one peak when aged for longer time. Partial DSC cycle runs were performed to identify the nature of these peaks. We found that the two peaks during cooling correspond to B2-R transformation and then R-B19′ transformation, respectively. The two peaks on heating for 1 h aged sample (Fig. 1(b)) correspond to B19′-R and R-B2 transformation, respectively; the one peak on heating for longer-time aged samples (Figs. 1(c)–(f)) corresponds to direct B19′-B2 transformation. The above is a normal transformation behavior for aged Ti–Ni alloys.

For aged 51.5Ni single crystal sample, DSC result is the same as the Ti–50.6Ni case (two peaks on cooling), except that for short-time (1 h) aged sample only one peak appears on both cooling and heating (Fig. 2(b)). From the small hysteresis in Fig. 2(b) we can conclude that this peak corresponds to B2-R transformation. The absence of R-B19′ transformation under such condition can be understood by considering that high Ni content of the sample results in high density of tiny precipitates in the B2 matrix; these fine precipitates are more effective in suppressing R-B19′ transformation than the B2-R transformation [3]. As the result, within our DSC temperature window there is only B2-R transformation. Except for being aged for short-time (1 h) Ti–51.5Ni sample show one-step B19′-B2 transformation on

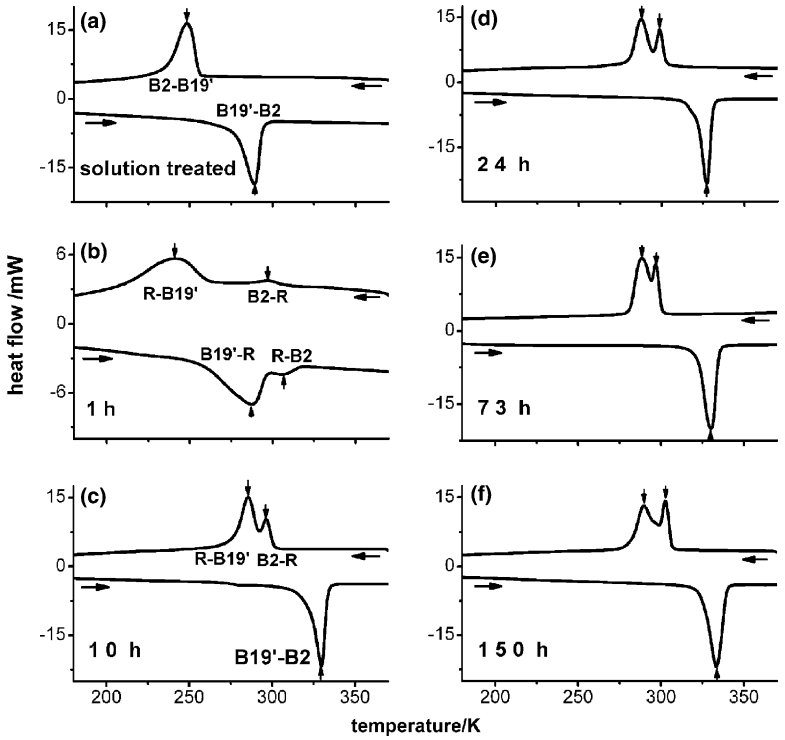

Fig. 1. DSC curves for Ti–50.6Ni single crystals: (a) solution-treated at 1273 K for 1 h followed by water quenching, (b–f) aged at 723 K for 1, 10, 24, 73, 150 h, respectively, after solution-treated at 1273 K for 1 h.

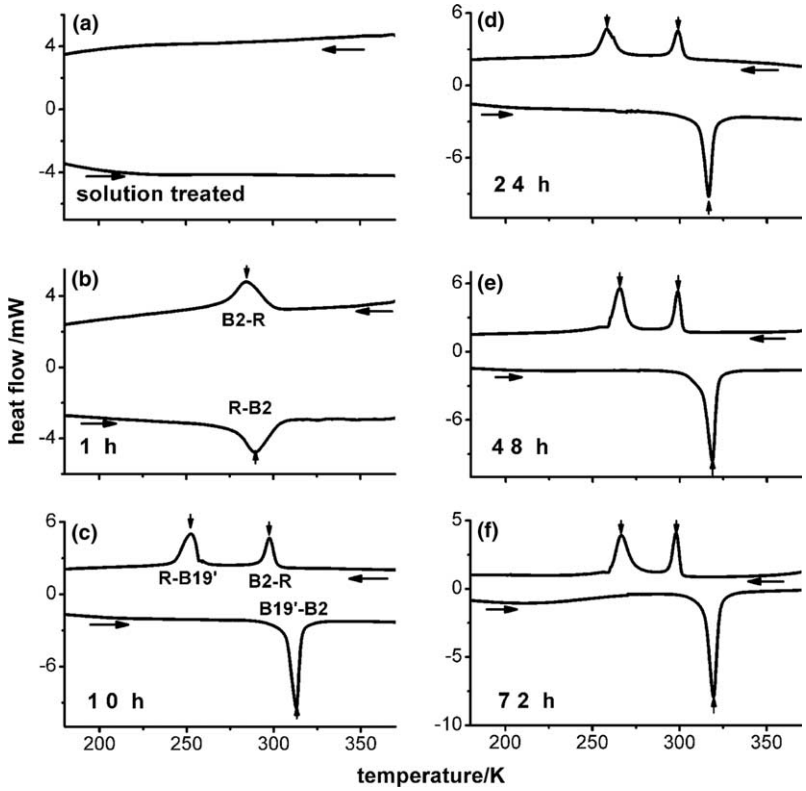

Fig. 2. DSC curves for Ti–51.5Ni single crystals: (a) solution-treated at 1273 K for 1 h followed by water quenching, (b–f) aged at 723 K for 1, 10, 24, 48, 72 h after solution-treated at 1273 K for 1 h.

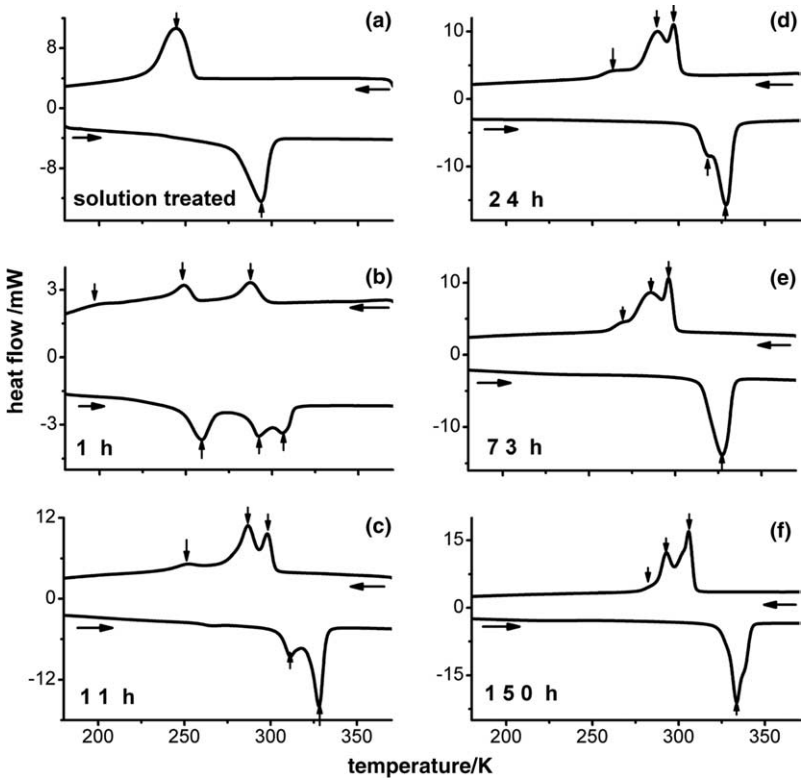

Fig. 3. DSC curves for Ti–50.6Ni artificial polycrystals: (a) solution-treated at 1273 K for 1 h followed by water quenching, (b–f) aged at 723 K for 1, 11, 24, 73, 150 h after solution-treated at 1273 K for 1 h.

heating (see heating curve of Figs. 2(c)–(f)), proved by partial-cycle DSC measurement.

DSC results of single crystal samples aged at other temperatures (from 573 to 773 K) are essentially the same as the above, i.e., there exist only two peaks on cooling (except that one pair of peaks on both cooling and heating is found for 51.5Ni sample when aged for short time. They correspond to B2-R and its reverse transformation).

Therefore, single crystals always exhibit normal two-stage (occasionally one-stage) transformation behavior, which was well documented in the literature for polycrystals. The abnormal three-stage transformation behavior was not found in single crystals of either low Ni (50.6Ni) or high Ni (51.5Ni) content. This important result has the implication that the abnormal three-stage behavior is not due to the small-scale stress- or composition-inhomogeneity around Ti_3Ni_4 particles, as such inhomogeneity would apparently exist even in these single crystals. The three-stage transformation behavior thus must be due to inhomogeneity over larger scale. This possibility will be explored in the following sections.

3.2. DSC results of artificial polycrystals

We now report the DSC curves for artificial polycrystals, which may have inhomogeneity over larger scale (i.e., between grain boundary and interior). As the artificial polycrystals have exactly the same composition as the corresponding single crystals as described above, a strict comparison between the two cases becomes possible.

Figs. 3(a)–(f) show the DSC curves of 50.6Ni artificial polycrystals. The DSC curve for solution-treated artificial polycrystal sample has no difference from that of single crystal sample (Fig. 3(a)). However, after aging at 723 K, DSC curve shows three peaks on cooling. With further increasing aging time, the third peak (low temperature peak) gradually shifts towards the second peak and finally merges into the second peak after long time aging. On heating artificial polycrystals show three peaks after short time aging (1 h), two after intermediate time aging (11, 24 h), and only one after long time aging.

For the high-Ni artificial polycrystal of 51.5Ni (Figs. 4(b)–(f)), DSC curves are the same as the corresponding single crystal results shown in Figs. 2(b)–(f) (except that the peaks appear broader in the polycrystal case). On cooling there is one peak for short-time aged sample and two peaks for longer-time aged samples. On heating only one-stage transformation was found for all the samples. As discussed in the previous section, this is a normal behavior: The first peak on cooling corresponds to B2-R transformation and the second peak corresponds to R-B19′ transformation. The single peak on heating corresponds to B19′-B2 direct transformation

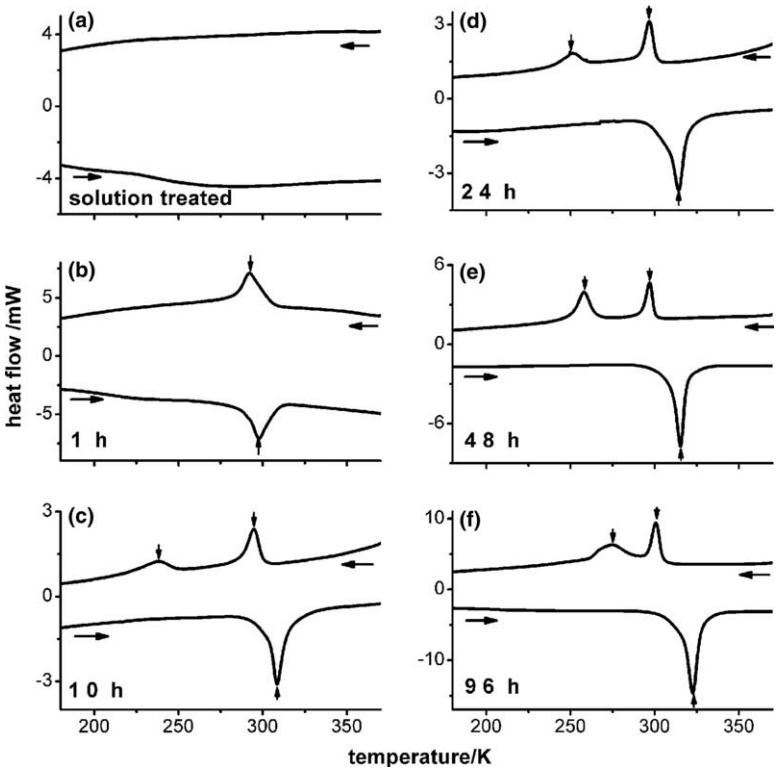

Fig. 4. DSC curves for Ti–51.5Ni artificial polycrystals: (a) solution-treated at 1273 K for 1 h followed by water quenching, (b–f) aged at 723 K for 1, 10, 24, 48, 96 h after solution-treated at 1273 K for 1 h.

(except for 1 h aged sample, which shows R-B2 one step transformation). Therefore, contrasting the 50.6Ni case three-stage martensitic transformation was never detected in all 51.5Ni polycrystal samples.

Therefore, the above results show that three-stage behavior is indeed related to the existence of grain boundary, as pointed out by Khalil-Allafi et al. [13] and Dlouhy et al. [14]; but grain boundary is not a sufficient condition for this behavior. Ni-content is another important factor, which has not been noticed so far. Three-stage behavior occurs only when Ni content is not high and in the presence of grain boundary. This new finding imposes new constraint for the possible mechanism.

3.3. Microstructure of aged artificial polycrystals by TEM observation

In order to understand the difference in transformation behavior between low Ni and high Ni artificial polycrystals, the microstructure of artificial polycrystals of different Ni content was characterized using TEM technique. The microstructures of a 50.6Ni artificial polycrystal sample aged at 723 K for 1 h is shown in Fig. 5(a). The key feature is that Ti_3Ni_4 particles form preferentially around grain boundary and much less in grain interior.

Fig. 5(b) shows the micrograph of a 51.5Ni artificial polycrystal sample aged at 723 K for 1 h. It can be clearly seen that a large number of small Ti_3Ni_4 particles were evenly distributed across the sample and do not show preference at the grain boundary. This is in sharp contrast to the Ti–50.6Ni case shown in Fig. 5(a).

Therefore, it becomes clear that grain boundary plays a key role in causing the inhomogeneous distribution of Ti_3Ni_4 precipitates; this is consistent with previous observations [13,14]. However, the new finding here is that the role of grain boundary is composition dependent, being ineffective when Ni content is high (e.g., 51.5Ni). This corresponds well to the contrasting transformation behavior of Ti–50.6Ni (Fig. 3) and Ti–51.5Ni (Fig. 4) artificial polycrystals.

3.4. Identifying the nature of three transformation stages of Ti–50.6Ni polycrystals by using partial DSC cycle runs

Now let us identify the nature of the three transformation peaks on cooling (Figs. 3(b)–(f)) of aged Ti–50.6Ni polycrystals. We have tried to directly observe the transformation across a grain by in situ TEM technique, but without success. The reason is that the thin film samples for TEM showed different transformation behavior from their bulk counterparts. In some cases, no transformation is observed although DSC data (of the bulk sample) clearly indicate transformation(s) occurs. Therefore, we abandoned using in situ TEM to identify the transformation nature, except for using it to

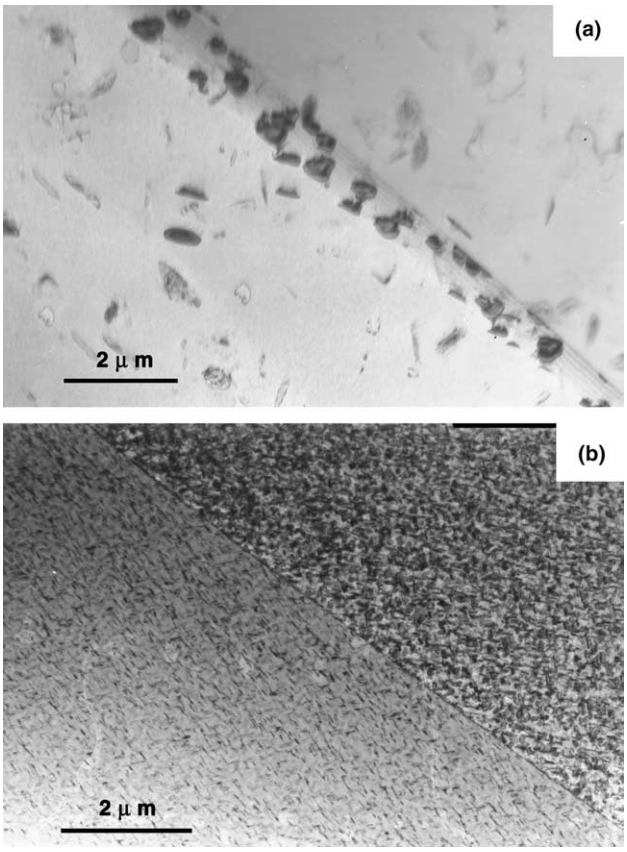

Fig. 5. TEM micrographs of artificial polycrystal samples after aging at 723 K for 1 h: (a) Ti–50.6Ni artificial polycrystal, (b) Ti–51.5Ni artificial polycrystal.

identify the distribution of Ti_3Ni_4 particles as shown in Fig. 5.

Therefore, we have to use a technique that can identify the nature of transformation in ''bulk state''. The technique we used is a ''partial DSC cycle technique'', which has been already used in the literature to identify the nature of multi-stage martensitic transformation [17]. The partial DSC cycle technique involves controlled cooling and heating to predefined temperatures, during which only selected transformation(s) is allowed to occur without triggering other transformations. By comparing with full DSC cycle data, one can determine the correspondence of heating and cooling peaks and the characteristics of each transformation such as hysteresis. From such information one can deduce the nature of each transformation.

Figs. 6 and 7 show the partial DSC cycle results of 50.6Ni artificial polycrystals aged at 723 K for 1 and 10 h, respectively. The full DSC cycles of both samples show three peaks during cooling, but there is a difference in the heating curve. The short-time (1 h) aged sample shows three peaks on heating (Fig. 6(a)) and longer-time (10 h) aged sample shows only two peaks on heating (Fig. 7(a)).

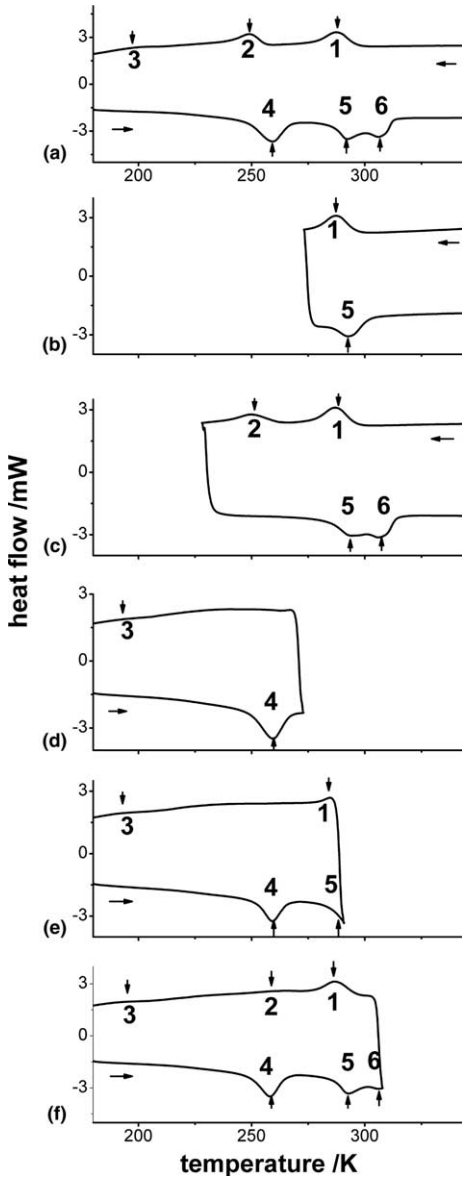

Fig. 6. Partial DSC cycles for Ti–50.6Ni artificial polycrystal sample after aging at 723 K for 1 h. The original full DSC curve of this sample has been shown in Fig. 3(b).

For 1 h aged 50.6Ni polycrystal sample, partial cycle Fig. 6(b) suggests that the cooling peak-1 corresponds to its reverse transformation peak-5. As this pair of peaks has only a narrow hysteresis of 2 K, we can deduce that it must be a B2-R transformation and its reverse transformation. From the microstructure of this sample shown in Fig. 5(a), which shows a segregation of Ti_3Ni_4 particles around grain boundaries, we can identify that peak-1 and peak-5 correspond, respectively, to the R-phase transformation and its reverse transformation of the grain boundary regions, as R-phase transformation occurs only in the presence of Ti_3Ni_4 particles. The partial cycle shown in Fig. 6(c) shows that with further cooling to trigger peak-2, the reverse transformation will

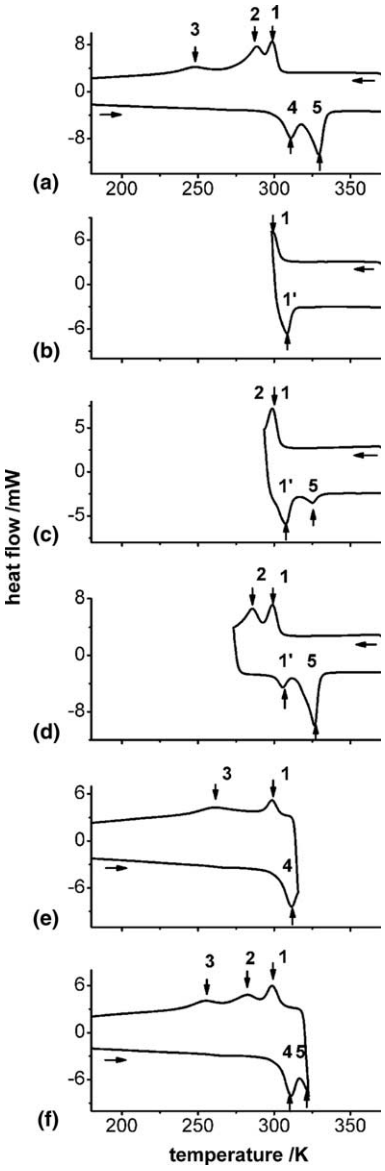

Fig. 7. Partial DSC cycles for Ti–50.6Ni artificial polycrystal sample after aging at 723 K for 10 h. The original full DSC curve of this sample has been shown in Fig. 3(c).

trigger peak-6, while both peak-1 and peak-5 are not affected. This clearly suggests that peak-2 and peak-6 is a pair of transformation, but occurs at different locations from grain boundaries. Then such transformation must be the transformation of the grain interior, where Ti_3Ni_4 particles are essentially free. From the large transformation hysteresis between peak-2 and peak-6, we can conclude that it must be a B2-B19′ transformation (and its reverse transformation) of this region. Partial cycle of Fig. 6(d) shows that when heating up from the lowest temperature to trigger only peak-4, the cooling transformation shows only peak-3 with peak-2 missing. Peak-2 appears only after heating to higher temperature to trigger peak-6, as shown in Fig. 6(f). This clearly indicates that peak-3 and peak-4 is a pair of transformation, which occurs in a different location from that responsible for peak-6. Apparently, peak-3 must be the R-B19′ transformation and peak-4 is its reverse transformation at the grain boundary region. This conclusion is also consistent with the wide hysteresis between peak-3 and peak-4.

Therefore, the whole transformation process of short-time aged Ti–50.6Ni artificial polycrystal sample can be summarized as the following:

1. *During cooling*:
   Peak-1: B2-R transformation of grain boundary region, where there is a high density of Ti_3Ni_4 particles.
   Peak-2: B2-B19′ transformation of the grain interior region, where Ti_3Ni_4 particles are essentially free.
   Peak-3: R-B19′ transformation of the grain boundary region.
2. *During heating*:
   Peak-4: B19′-R transformation of the grain boundary region.
   Peak-5: R-B2 transformation of the grain boundary region.
   Peak-6: B19′-B2 transformation of the grain interior region.

For longer-time (10 h) aged Ti–50.6Ni sample, the partial cycles (Figs. 7(b)–(f)) indicate that peak-1 and peak-3 correspond to peak-4, and peak-2 corresponds to peak-5. By the same reasoning we can conclude the sequence of the transformation as the following:

1. *During cooling*:
   Peak-1: B2-R transformation of grain boundary region.
   Peak-1′: R-B2 reverse transformation of grain boundary region.
   Peak-2: B2-B19′ transformation of the grain interior region, where Ti_3Ni_4 particles are essentially absent.
   Peak-3: R-B19′ transformation of the grain boundary region.
2. *During heating*:
   Peak-4: B19′-B2 transformation of the grain boundary region.
   Peak-5: B19′-B2 transformation of the grain interior region.

4. Discussions

4.1. A unified explanation for both three-stage transformation and two-stage transformation in Ti–Ni polycrystals

Our results in the preceding sections have demonstrated two key points, which will be the basis for understanding both three-peak behavior and two-peak behavior of Ti–Ni alloys.

Firstly, the non-existence of three-stage transformation behavior in aged Ti–Ni *single crystals* clearly demonstrates that small-scale stress or composition

inhomogeneity around Ti_3Ni_4 particles is not responsible for the three-stage behavior, as such kind of inhomogeneity definitely exists in single crystals. This excludes those mechanisms based on small-scale inhomogeneity around precipitates, and suggests that three-stage transformation behavior should be due to inhomogeneity over larger scale, possibly associated with grain boundary effect.

Secondly, polycrystal sample of low-Ni (50.6Ni) shows three-peak behavior whereas high-Ni sample (51.5Ni) demonstrates normal two-peak behavior. Our TEM results (Fig. 5) and the corresponding DSC results (Figs. 3 and 4) clearly showed such difference depends on if there is inhomogeneous distribution of Ti_3Ni_4 over large scale (i.e., between grain boundary and interior).

The above points indicate that the presence of grain boundary is a necessary condition for three-peak behavior, but it is not a sufficient condition. The transformation behavior is dependent on how Ti_3Ni_4 particles are distributed between grain boundary and grain interior. Then the central question here is: "what determines a homogeneous or heterogeneous distribution of Ti_3Ni_4 precipitates in polycrystals?" The answer to this question will naturally explain the origin of the three-stage transformation.

In the following we shall show that the contrasting behaviors of 50.6Ni and 51.5Ni polycrystal samples are actually determined by a single governing principle, that is, kinetics of precipitation in *polycrystalline* supersaturated solid solutions. Before considering the effect of grain boundary, we first consider the case of homogeneous nucleation. In Ni-rich (supersaturated) Ti–Ni alloys, Ti_3Ni_4 precipitates in B2 matrix during aging, and Ni content of matrix decreases until reaching equilibrium Ni content [18]. According to the theory of phase transformation kinetics [19], nucleation rate I (the number of stable nuclei formed in the assembly in unit time) can be written as

$$I \propto \exp(-\Delta G_c/kT), \tag{1}$$

where ΔG_c is the critical free energy to form a nucleus (i.e., nucleation barrier); k is the Boltzmann constant; T is transformation temperature. This equation shows that nucleation rate is determined by nucleation barrier ΔG_c.

The nucleation barrier ΔG_c for coherent nuclei is given by [20]

$$\Delta G_c = 16\pi\sigma^3/[3(\Delta G_v + \varepsilon)^2], \tag{2}$$

where ΔG_v is the chemical free energy change associated with the precipitation reaction, ε is the strain energy per unit volume associated with the formation of a nucleus, σ is the interfacial energy associated with the formation of the new interface. Here it should be noted that ΔG_v is the driving force for the formation of new phase and thus must be negative to enable the precipitation to happen. This requires that the solid solution must be supersaturated, i.e, solute concentration must be beyond its solubility limit in the solid solution (this situation is produced by rapid cooling of more concentrated solid solution from higher temperature, as being the case for our quenched Ti–Ni alloys). The larger the degree of supersaturation (i.e., the excess solute concentration beyond solubility limit) the more negative is the driving force ΔG_v for precipitation. According to Eq. (2), at small supersaturation or small driving force ΔG_v the nucleation barrier ΔG_c will reach infinite; thus from Eq. (1) we know that nucleation rate is virtually zero. At very large supersaturation or large driving force ΔG_v, the nucleation barrier ΔG_c is almost zero and thus the nucleation rate will reach a high plateau following Eq. (1). Therefore, the typical form of nucleation rate as a function of supersaturation or driving force will be a step-like curve as schematically shown in Fig. 8 (Fig. 8 uses supersaturation ΔX as horizontal axis to provide easier link to the composition of alloys). It is characterized by an almost zero nucleation rate at small supersaturation/driving-force and rapid increase with increasing supersaturation until reaching a constant level at large supersaturation.

Now we consider the effect of grain boundary. In the case of polycrystals, at grain boundary (or similar defect) nucleation barrier is much reduced compared with that at grain interior. It was shown that nucleation barrier could become a fraction of that for homogeneous nucleation [19]. For a qualitative evaluation of the effect of grain boundary, let us assume there is a half reduction of the nucleation barrier, $\Delta G_c^{GB} = (\Delta G_c)/2$; then one can easily conclude from Eq. (1) that the nucleation rate curve for grain boundary (I_{GB}) will be shifted to left side compared with that for grain interior (I_{GI}), where homogeneous nucleation occurs. Fig. 8 shows that at low supersaturation grain boundary

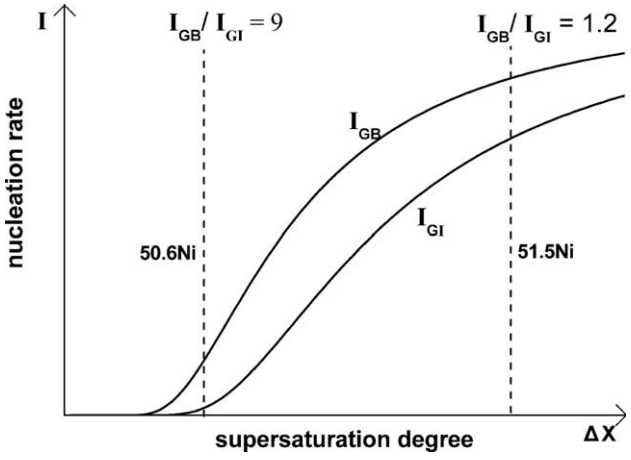

Fig. 8. Schematic illustration for the relation between nucleation rate and supersaturation degree in grain interior region and grain boundary region. Supersaturation degree ΔX is defined by the solute (Ni) concentration beyond its solubility limit in B2 Ti–Ni phase at given aging temperature. The nucleation rate at grain boundary and at grain interior is indicated by I_{GB} and I_{GI}, respectively.

nucleation rate is significantly larger than that of grain interior; but at high supersaturation there is not a large difference. As will be seen below, this is an important feature and explains what we observed experimentally.

Fig. 8 answers the question about what determines whether there should be a preferential precipitation at grain boundary or an essentially homogeneous precipitation. When Ni content is low (50.6Ni), the nucleation rate is very small and thus precipitation of Ti_3Ni_4 is very sensitive to the presence of grain boundary. In this case, nucleation rate at grain boundary is much larger than at grain interior, as shown in Fig. 8. As a result, precipitation mainly occurs at grain boundary and grain interior is essentially precipitate-free. When Ni content is high (51.5Ni), the difference in nucleation rate between grain boundary and interior is small; thus precipitation occurs homogeneously without being affected by grain boundary, as shown in Fig. 8. As a result, high supersaturation or high Ni content favors a homogeneous distribution of precipitates.

Therefore, there are two competing factors, which control the resultant distribution of precipitates in Ni-rich Ti–Ni alloys. The first factor is the presence of grain boundary or similar defects, which favors a preferred precipitation along grain boundaries. The second factor, which has an opposite effect, is the degree of supersaturation of Ni (or Ni content). The competition between the two factors determines whether there will be a heterogeneous or a homogeneous distribution of precipitates.

After understanding what determines whether there will be a heterogeneous or homogeneous distribution of Ti_3Ni_4, now it is very easy to understand the different transformation behaviors of low Ni and high Ni Ti–Ni polycrystals. This is shown in Fig. 9. For low-Ni samples, the low supersaturation leads to a preferential precipitation along grain boundary (Figs. 9(a) and (b)) where leaving grain interior essentially precipitate-free, as discussed above. So grain boundary portion undergoes B2-R-B19′ two-stage transformation while the grain interior, being free of precipitates, undergoes a direct B2-B19′ transformation and this gives rise to totally three-stage transformation. For high Ni content alloys, as the supersatuation is high there is no much difference in nucleation rate between grain boundary and grain interior; thus an essentially homogeneous distribution of precipitates is obtained across the whole sample, without being affected by grain boundaries. So the whole sample undergoes normal two-stage transformation. Therefore, both abnormal three-peak behavior and normal two-peak behavior can find a unified and natural explanation by the theory of precipitation kinetics.

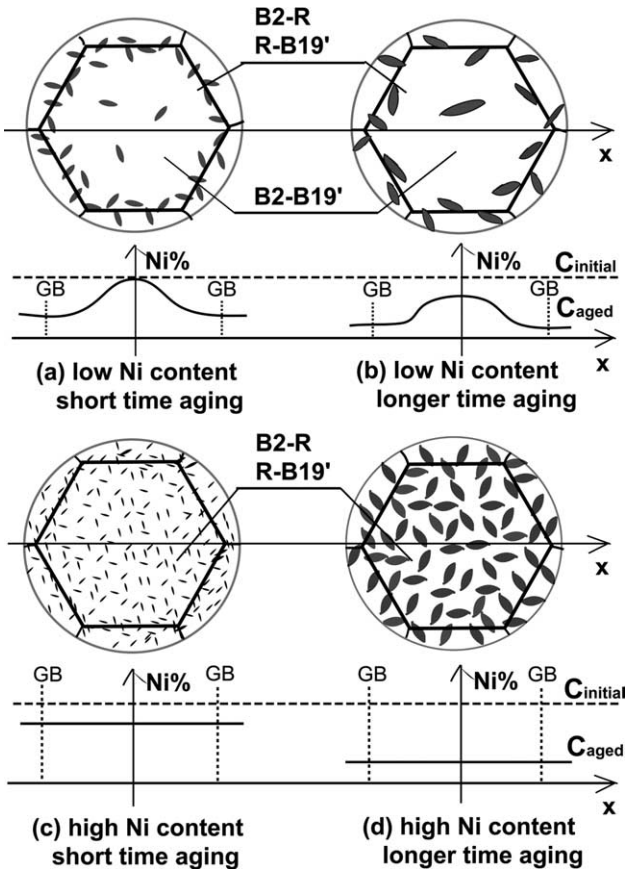

Fig. 9. A unified model for explaining the microstructure evolution at low Ni supersaturation (a and b) and high Ni supersaturation (c and d). It also explains both three-stage and two-stage transformation behavior of supersaturated Ti–Ni solid solution. In the figure, $C_{initial}$ and C_{aged} curves represent the Ni profile of initial (as-quenched) state and that after aging, respectively. GB denotes grain boundary.

4.2. The evolution of DSC peaks with aging time

Our model (Fig. 9) can also explain the evolution of DSC peak positions with aging time. When the low Ni polycrystal is aged for short time (1 h), only a small amount of Ti_3Ni_4 particles of small size precipitate at grain boundary; the grain interior region is essentially free of Ti_3Ni_4 particles (Fig. 9(a)) and thus grain interior has the same composition as the solution-treated state. As a consequence the grain interior undergoes one-stage transformation $B2_{GI} \rightarrow B19'_{GI}$ and its transformation temperature should be the same as that of solution-treated sample. Fig. 3 shows this is really the case; in this figure the second peak on cooling (which corresponds to the $B2_{GI} \rightarrow B19'_{GI}$ transformation) for 723 K for 1 h aged sample (Fig. 3(b)) is found to be in the same position as the cooling peak of the solution-treated sample (Fig. 3(a)). At grain boundary region, precipitation causes a decrease in Ni concentration in the B2 matrix and this favors an increase in R-B19′ transformation; however, the presence of small Ti_3Ni_4 particles produces a strong resistance to large lattice deformations associated with the formation of B19′. Therefore, the transformation temperature for $R_{GB} \rightarrow B19'_{GB}$ is even lower than that of $B2_{GI} \rightarrow B19'_{GI}$.

As aging time increases, Ti_3Ni_4 particles grow larger by consuming other small Ti_3Ni_4 particles and absorb Ni from the supersaturated particle-free grain interior region. So both Ni concentrations (C_{aged}) in grain boundary region and particle-free grain interior region decrease with aging time (in Fig. 9(b)). At the same time precipitates also grow and the spacing becomes larger. These widely spaced particles then produce relatively small resistance to the formation of B19′ [18]; so the transformation temperature of $R_{GB} \rightarrow B19'_{GB}$ increases rapidly with aging time. However, the formation temperature of R-phase mainly depends on the Ni concentration in the matrix and is less affected by particle size; so the transformation temperature of $B2_{GB} \rightarrow R_{GB}$ does not increase significantly even after prolonged aging (Figs. 3(b)–(f)). The second peak of $B2_{GI} \rightarrow B19'_{GI}$ transformation also increases with aging time because of the decreasing Ni concentration in the B2 matrix as mentioned above. During this process the volume of the precipitate-free grain interior also increases as a result of the decreasing number of Ti_3Ni_4 particles. Thus transformation heat associated with $B2_{GI} \rightarrow B19'_{GI}$ transformation increases. This is consistent with the experimental fact in Fig. 3 that the peak-2 becomes larger with increasing aging time. At the same time the peaks for $B2_{GB} \rightarrow R_{GB}$ and $R_{GB} \rightarrow B19'_{GB}$ become smaller. When the aging time is further increased, Ni concentration in the matrix reaches equilibrium. The transformation temperature of $B2_{GI} \rightarrow B19'_{GI}$ will no longer change with aging time. However, Ti_3Ni_4 particles still grow larger by consuming other small Ti_3Ni_4 particles, so the temperature of $R_{GB} \rightarrow B19'_{GB}$ transformation still gradually increases with aging time and finally reaches the temperature of $B2_{GI} \rightarrow B19'_{GI}$ transformation and the two peaks merge into one. On heating the peaks evolve with aging time in a similar way and finally the two peaks of $B19'_{GB} \rightarrow B2_{GB}$ and $B19'_{GI} \rightarrow B2_{GI}$ become one peak after long time aging.

For high Ni-content polycrystals the Ti_3Ni_4 particles are evenly distributed across the whole samples under all aging conditions (Figs. 9(c) and (d)), without being affected by grain boundary. This is the same as the case of single crystals. Thus the whole sample undergoes two-stage transformation on cooling after aging (one stage after short-time aging), in the same way as the corresponding single crystal.

Finally, it should be noted that the sequence of the transformations may vary with composition and aging temperature, as these two factors strongly affect nucleation rate.

4.3. Other factors that may cause three-stage transformation

Some other factors may also cause three-stage transformation by promoting the preferential precipitation around grain boundary. Ti is known to be apt to be oxidized. If Ti–Ni samples are heat treated in the air or in low vacuum atmosphere such as conventional vacuum or Ar sealing practices), the Ti atom at grain boundary may easily react with O_2, which results in excess Ni at the grain boundary. Higher concentration of Ni at grain boundary makes it easier for Ni-rich Ti_3Ni_4 particles to precipitate at grain boundary, thus leading to a three-stage transformation. If the sample is protected by Ti getter from oxidation at grain boundary, heterogeneous precipitation of Ti_3Ni_4 particles at grain boundary may be avoided and this gives rise to homogeneous precipitation and consequently normal two-stage transformation. This explains the finding by Nishida et al. [16] that transformation behavior is also dependent on atmosphere during heat treatment.

5. Conclusions

To clarify the basic mechanism that controls the peculiar three-stage martensitic transformations in aged Ni-rich Ti–Ni alloys, we investigated Ti–50.6Ni and Ti–51.5Ni single crystals and their corresponding ''artificial polycrystals'' (which were made from single crystals of the same composition) by using DSC and TEM techniques, and obtained the following conclusions.

(1) All aged single crystals exhibit normal B2-R-B19′ two-stage transformation, being independent of Ni content of the alloy. i.e. Single crystals do not exhibit three-stage transformation, which were reported previously for polycrystals. This suggests that local stress or composition inhomogeneity around Ti_3Ni_4 is not responsible for the abnormal three-stage transformation.

(2) On the contrary, aged artificial polycrystals with low Ni content (50.6Ni) exhibit a three-stage transformation; but those with high Ni content (51.5Ni) again exhibit a normal two-stage transformation. These results have the important implication that the introduced grain boundaries are responsible for three-stage transformation, but it is not a sufficient condition.

(3) To account for these phenomena in both single crystals and polycrystals of different Ni content, we proposed a simple model that different transformation behaviors are a result of competition between preferential grain boundary precipitation of Ti_3Ni_4 particles and a tendency for homogeneous precipitation when supersaturation of Ni is large.

(4) Basically the abnormal three-stage transformation is due to preferential precipitation of Ti_3Ni_4 particles at grain boundary, which generates *large-scale* heterogeneity in microstructure and chemical composition between grain boundary and interior. Grain boundary region undergoes B2-R-B19′ two-stage transformation, while the grain interior, being free of precipitates,

undergoes a direct B2-B19′ transformation; thus there are in total three transformation stages. On the contrary, when Ni content is high, the large supersaturation of Ni in quenched Ti–Ni alloy provides a large driving force for the precipitation of Ti_3Ni_4 particles during aging and this makes the formation of precipitates less sensitive to grain boundaries and results in a relatively homogeneous precipitation. As the consequence, normal two-stage B2-R-B19′ transformation occurs for polycrystalline Ti–Ni of high Ni content, being the same as in single crystals.

(5) Our model also explains other features observed in DSC experiments, such as the evolution of DSC peak positions with aging time, as well as the reported dependence of the transformation behavior on heat-treatment atmosphere.

Acknowledgements

The authors thank Yu.I. Chumlyakov for providing single crystal samples, Jun Sun, Shengtao Li, Xiangdong Ding, Quncheng Fan, T. Suzuki for helpful discussions, K. Nashida for EPMA chemical analysis of the samples. This work was supported by Sakigaki-21 of JST and a special fund for Cheungkong Professorship and National Natural Science Foundation of China.

References

[1] Otsuka K, Wayman CM, editors. Shape memory materials. Cambridge: Cambridge University Press; 1998.
[2] Van Humbeeck J. Mater Sci Eng A 1999;273–275:134–48.
[3] Ren X, Miura N, Taniwaki K, Otsuka K, Suzuki T, Tanaka K, et al. Mater Sci Eng A 1999;273–275:190.
[4] Stroz D, Kwarciak J, Morawiec H. J Mater Sci 1988;23:4127.
[5] Stroz D, Bojarski Z, Ilczuk J, Lekston Z, Morawiecz H. J Mater Sci 1991;26:1741.
[6] Meisel LV, Cote PJ. Miner Met Mater Soc 1992;1:17.
[7] Morawiecz H, Stroz D, Chrobak D. J Phys 1995;4:C2–C205.
[8] Bataillard L, Gotthardt R. J Phys IV 1995:C8–C647.
[9] Morawiec H, Stroz D, Goryczka T, Chrobak D. Scr Mater 1996;35:485.
[10] Morawiec H, Ilczuk J, Stroz D, Goryczka T, Chrobak D. J Phys IV 1997;4646:C5–C155.
[11] Bataillard L, Bidaux J-E, Gotthardt R. Philos Mag 1998;78:327.
[12] Khalil-Allafi J, Ren X, Eggeler G. Acta Mater 2002;50:793.
[13] Khalil-Allafi J, Dlouhy A, Eggeler G. Acta Mater 2002;50:4225.
[14] Dlouhy A, Khalil-Allafi J, Eggeler G. Philos Mag 2003;83:339.
[15] Sitepu H, Schmahl WW, Allafi JK, Eggeler G, Dlouhy A, Toebbens DM, et al. Scr Mater 2002;46:543–8.
[16] Nishida M, Hara T, Ohba T, Yamaguchi K, Tanaka K, Yamauchi K. Mater Trans 2003;44:2631–6.
[17] Favier D, LiuY, McCormick PG. Scr Metall Mater 1992;28:669–72.
[18] Zhang J, Cai W, Ren X, Otsuka K, Asai M. Mater Trans JIM 1999;40:1367.
[19] Christian JW. The theory of transformations in metals and alloys, part 1. Oxford: Pergamon Press; 2002. p. 422–79.
[20] Russell KC. Phase transformations. Ohio: ASM; 1969. p. 219–68.